

## Oxidative Degradation of Nadic-End-Capped Polyimides. 2. Evidence for Reactions Occurring at High Temperatures

Mary Ann B. Meador\* and J. Christopher Johnston

Materials Division, NASA Lewis Research Center, Cleveland, Ohio 44135-3191

Paul J. Cavano

Department of Chemistry, Case Western Reserve University, Cleveland, Ohio

Aryeh A. Frimer<sup>1,2</sup>

Department of Chemistry, Bar-Ilan University, Ramat Gan 52900, Israel

Received January 27, 1997<sup>o</sup>

**ABSTRACT:** The oxidative degradation of PMR (for olymerization of monomeric reactants) polyimides at elevated temperatures was followed by cross-polarized magic angle spinning (CP-MAS) NMR. <sup>13</sup>C labeling of selected sites in the polymers allowed for direct observation of the transformations arising from oxidation processes. As opposed to model compound studies, the reactions were followed directly in the polymer. The labeling experiments confirm the previously reported oxidation of the methylene carbon to ketone in the methylenedianiline portion of the polymer chain. They also show the formation of two other oxidized species, acid and ester, from this same carbon. In addition, the technique provides the first evidence of the kind of degradation reactions that are occurring in the nadic end caps. Several PMR formulations containing moieties determined to be present after oxidation, as suggested by the labeling study, were synthesized. Weight loss, FTIR, and natural abundance NMR of these derivatives were followed during aging. In this way, weight loss could be related to the observed transformations.

### Introduction

Norbornenyl-end-capped PMR (for polymerization of monomeric reactants) polyimide resins<sup>3</sup> are some of the most widely used polymer matrix composite materials for aircraft engine applications,<sup>4</sup> since they combine ease of processing with good oxidative stability up to 300 °C. These PMR resins are prepared by a novel approach involving the initial formation of oligomeric prepolymers capped at both ends by a reactive end cap. The end cap undergoes cross-linking during processing, producing the desired low-density, high-specific-strength materials. For example, the classic preparation of PMR-15 (Scheme 1) involves the initial formation of a polyimide prepolymer via the 200–250 °C condensation of three monomer reactants: 4,4'-methylenedianiline (MDA, **1**), the dimethyl ester of benzophenone-3,4,3',4'-tetracarboxylic 3,4:3'4'-dianhydride (BTDE, **2**), and 2-carbomethoxy-3-carboxy-5-norbornene (the monomethyl ester of nadic diacid, NE, **3**).<sup>2</sup> This results in a polyimide oligomer with a formulated molecular weight of approximately 1500 g/mol—hence, the acronym PMR-15. This oligomer has a low enough melt viscosity to allow the volatile byproducts of the condensation reaction to escape before it undergoes cross-linking through the nadic end cap at 275–325 °C, producing a void-free network structure. There is also a final postcure that generally raises the glass transition temperature (*T*<sub>g</sub>) of the resin.

Much of the research on neat resins and polymer matrix composites over the past two decades has been focused on improving both the thermal oxidative stability (TOS) and performance of these materials. Directions that have been explored in the PMR-type systems include higher molecular weight formulations (and, hence, lower relative amounts of end cap), alternate anhydrides or diamines (e.g., PMR-II<sup>5</sup>), more stable end caps (e.g., V-cap<sup>6</sup>), and various postcuring techniques

(e.g., nitrogen postcuring<sup>7</sup>).

Despite the advances made in the area of TOS, only slow progress has been made in understanding the source and mechanism of the physical and chemical changes that occur during thermal and oxidative degradation. Several pieces of the puzzle do exist, however:

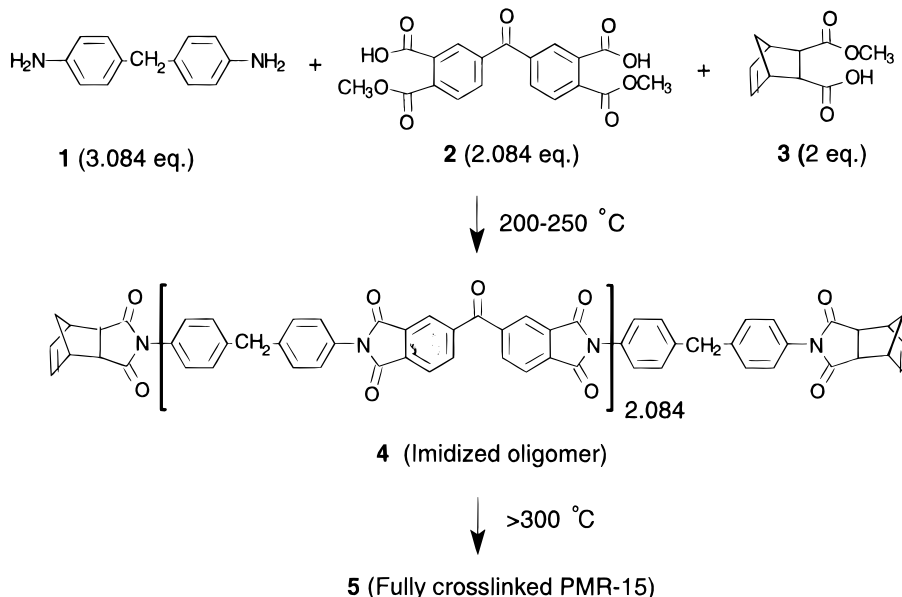
(1) There are substantial Fourier transform infrared spectroscopy (FTIR) data indicating that, in PMR-15 and related analogs, the dibenzylmethylene group of MDA undergoes oxidation during aging to the corresponding benzophenone.<sup>8</sup> This transformation, however, cannot be the direct source of the weight loss observed, since carbonyl formation should actually result in a weight gain and in a structure more resistant to oxidation.

(2) The end cap is what makes these polyimides more processable compared to corresponding condensation polymers. Unfortunately, norbornenyl-end-capped polyimides are known to undergo weight loss faster on high-temperature aging than non-end-capped polyimides with the same backbone.<sup>9</sup> Nevertheless, with no strong characteristic peaks due to the end cap in the FTIR, little has been said in the literature<sup>8c,e,f</sup> about the mechanism of this degradation.

(3) Synthetic<sup>10</sup> and thermogravimetric analysis (TGA)<sup>11</sup> work by Frimer *et al.* suggests that thermolysis of the relatively weak (bond dissociation energy, 50–65 kcal/mol) imide bond is involved in the degradation.

(4) Thermally-generated free radicals have been found in room-temperature electron paramagnetic resonance (EPR) studies of PMR-15 and other polyimides, exposed to elevated temperatures above 300 °C.<sup>12</sup> There are at least two different types of free radicals persistent at room temperature in PMR-15, one arising from the imide moiety. Correlation between weight loss and free radical concentration suggests that the radicals are directly involved in degradation of the polyimides in the presence of air.

<sup>o</sup> Abstract published in *Advance ACS Abstracts*, May 15, 1997.

**Scheme 1. Synthetic Scheme for the Preparation of PMR-15**

(5) Bowles and co-workers<sup>13</sup> have observed that oxidation of PMR-15 neat resin, aged at temperatures up to 343 °C for 3000 h, occurs in a narrow surface layer only 0.1–0.2 mm thick. Voids form in this layer, and with continued exposure, surface cracks develop, exposing more of the interior of the sample.

(6) In this regard, Meador and co-workers<sup>8g,h</sup> report microscopic FTIR evidence of differences in the chemical composition of the oxidation layer and the interior of the sample. The spectrum of the interior is unchanged from that of as-processed PMR-15, while that of the oxidation layer is consistent with the aforementioned oxidation of the MDA methylene to the corresponding carbonyl. In addition, peaks attributed to the end-cap skeleton are nearly gone in the FTIR spectrum of the oxidation layer.

(7) Meador *et al.*<sup>8g,h</sup> also found no significant effect of thermocycling on the weight loss of PMR-15 neat resins. Temperature had the strongest effect on weight loss of all the variables studied. At a given temperature, initial weight loss rates were higher than those near the end of the test. This is consistent with either parabolic or parabolic kinetics. Their data and Bowles<sup>13</sup> suggest the following oxidative attack scenario: An initial oxygenation of the surface leads to the formation of volatile and nonvolatile products. The nonvolatile products remain attached to the underlying material, forming a reaction zone that tends to increase with time. As the zone thickens, the reaction rate decreases as either the inward diffusion of oxygen or the outward diffusion of the gaseous product(s) becomes rate limiting. As the thermal degradation continues and the diffusion path increases, the oxygen/solid reaction slows. At some point, the rate of reaction zone lost at the surface becomes equal to the rate of reaction zone formed. As a result, the thickness of the zone and the weight loss rate become constant.

Briefly summarizing, then, due to the complexity of the problem and the limitations of the analytical techniques used, only certain aspects of the degradation have been observed. Consequently, an overall understanding of the mechanism is still lacking. Thus, the purpose of this study is to more fully identify the chemical changes that occur during the high-tempera-

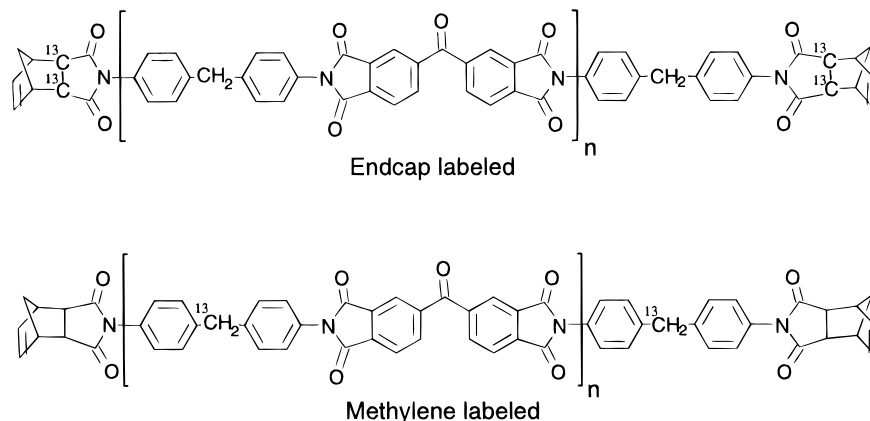
ture oxidation with particular focus on the norbornenyl end caps.

This paper presents direct spectral evidence for some of the molecular level changes occurring on thermal oxidative aging of these polyimides. The changes were followed by <sup>13</sup>C NMR of solid samples. Polymers were prepared enriched with <sup>13</sup>C in specific sites to follow changes occurring at those particular carbons as aging proceeds.<sup>14</sup> This provides more easily interpretable evidence than FTIR or natural abundance <sup>13</sup>C NMR. Several PMR formulations containing moieties determined to be present after oxidation, as suggested by the <sup>13</sup>C-labeling study, were synthesized. Weight loss, FTIR, and natural abundance NMR of these derivatives were followed during aging. In this way, weight loss could be related to the observed transformations.

## Experimental Section

**(1) General.** Benzophenonetetracarboxylic dianhydride (**2**, BTDA, 98%), 4,4'-diaminobenzophenone (DABP, 97%), 4,4'-methylenedianiline (**1**, MDA, 97%), 5-norbornene-2,3-dicarboxylic anhydride (also dubbed nadic anhydride, NA, 98%), and phthalic anhydride (PA, 99+%) were purchased from Aldrich Chemical Co. (Milwaukee, WI). 5-Norbornene-2,3-dicarboxylic acid monomethyl ester (**3**, nadic ester, NE, 98%) was obtained from Chriskev Chemical Company (Leawood, KS). <sup>13</sup>C isotope-labeled 4,4'-methylenedianiline and 5-norbornene-2,3-dicarboxylic anhydride (labeled at the methylene carbon and  $\alpha$  to the carbonyl groups, respectively; see Scheme 2) were obtained from Isotec (Miamisburg, OH). All the above commercially available chemicals were used without further purification.

**(2) General Procedures for the Preparation of Imidized Oligomers (Molding Powders) of PMR-15 and Derivatives.** Molding powders were synthesized using the procedures exemplified below for PMR-19 (formulated molecular weight of 1900 g/mol) and DABP-15 (the DABP analog of PMR-15). The differences in these procedures result from the relative insolubility of DABP and its oligomers in CH<sub>3</sub>OH. In addition, because of the electron-withdrawing carbonyl in DABP, the amino groups are less nucleophilic, and more stringent conditions are required for complete imidization. The number of moles of monomeric reactants in each case was governed by the ratio  $n/(n+1)/2$ , where  $n$ ,  $(n+1)$ , and 2 are the number of moles of dianhydride (BTDA), diamine (MDA or DABP), and end cap (NE or phthalic acid monomethyl ester, PE), respectively. The two examples given below utilize

Scheme 2. Two  $^{13}\text{C}$ -Enriched Modifications of PMR-15

commercially available NE as the end cap directly. However, when PE or  $^{13}\text{C}$ -labeled NE was used as the end cap, it was generated *in situ* by refluxing the corresponding anhydride together with the BTDA. The molding powders, determined to be fully imidized on the basis of FTIR and thermal analysis, were ground to fine powders prior to use in resin formation.

**(3) PMR-19 ( $n = 3$ ).** BTDA (19.32 g, 0.06 mol) and  $\text{CH}_3\text{OH}$  (100 mL) were combined in a 500 mL bottle with a stirring bar. The suspension was heated to boiling for ca. 1.5 h (approximately 1 h after dissolution of the dianhydride) in order to convert the BTDA to the corresponding diacid–diester (BTDE). MDA (15.86 g, 0.08 mol) and NE (7.85 g, 0.04 mol) were added, and the mixture was stirred and heated to boiling until all the diamine dissolved. The solution was then concentrated on a hot plate, and evaporation of the solvent continued until a thick syrup was obtained. The stirring bar was removed, and the syrup was spread on the walls of the bottle by rolling the bottle on the hot plate to remove the remaining solvent. The resulting foam was crushed and imidization was completed by heating the sample at 200 °C (rise time, 1 h; dwell time, 1 h) and 230 °C (rise time, 0.5 h; dwell time, 0.5 h) to give 38.63 g.

**(4) DABP-15 ( $n = 2$ ).** BTDA (12.89 g, 0.04 mol),  $\text{CH}_3\text{OH}$  (300 mL), and a stirring bar were combined in a 1000 mL Erlenmeyer flask. After the suspension was boiled for ca. 1.5 h (see above), DABP (12.74 g, 0.06 mol), NE (7.85 g, 0.04 mol), and  $\text{CH}_3\text{OH}$  (to a total of 850 mL of solution) were added. Boiling was continued until all the diamine dissolved. The solution was then concentrated on a hot plate to 400 mL and transferred to a 500 mL glass bottle. At about 350 mL, a precipitate formed. The solvent was concentrated to about 100 mL, the stirring bar was removed, and evaporation of the solvent was continued until a thick syrup was obtained. The syrup was spread on the walls of the bottle by rolling the bottle on the hot plate to remove the remaining solvent. The resulting foam was crushed, and imidization was completed by heating the sample at 200 °C (rise time, 1 h; dwell time, 1 h), 230 °C (rise time, 0.5 h; dwell time, 0.5 h), and 260 °C (rise time, 0.5 h; dwell time, 0.5 h) to give 29.21 g.

**(5) Preparation of  $^{13}\text{C}$ -Labeled Oligomers.** Synthesis of the isotope-labeled imidized oligomers, and the unlabeled oligomers used for direct comparison, was carried out on a 1.5 g scale. In a typical procedure, NA (0.328 g, 2 mmol; 0.332 g if labeled) and BTDA (0.672 g, 2.084 mmol) were refluxed in  $\text{CH}_3\text{OH}$  (5 mL) for 2 h. The clear solution was cooled, and MDA (0.611 g, 3.084 mmol; 0.614 g if labeled) was added. The  $\text{CH}_3\text{OH}$  was removed from the resulting yellow solution by rotary evaporation at 35 °C to give a yellow foam. The foam was gently crushed to a coarse solid that was imidized in an air-circulating oven at 200 °C for 2 h followed by 0.5 h at 230 °C. The dark yellow solid was finely ground with mortar and pestle to give the fully imidized molding powder, as evidenced by thermal analysis, liquid chromatography, NMR, and FTIR.

**(6) Neat Resin Molding.** A 1.27 cm (0.5 in.) inside-diameter hardened tool-steel die was used for all disk moldings. A 10 cm  $\times$  10 cm (4 in.  $\times$  4 in.; inside dimensions) die was used to prepare neat resin rectangular plates. Mold

surfaces were treated with a silicone-containing commercial release agent (Frecote-44, Dexter Corporation). A hydraulic press with electrically heated platens and a maximum capacity of 12 tons was used to apply pressure and provide heat to the molding tool.

Prior to molding, imidized oligomers were examined by thermal gravimetric analysis (TGA) and differential scanning calorimetry (DSC) techniques to identify major transitions and any unusual weight loss events. Mold cycle final temperature, rise rate, and pressure conditions were based on these results and a knowledge of unmodified PMR-15 molding powder from various sources.

**(a) Disks.** In a typical resin disk preparation, press platens were preheated to 280 °C, and a cold die containing the molding powder was placed in the press. A charge weight of 0.3–0.4 g of molding powder was typical. To permit the release of any residual evolved gas, mechanical stops were initially used to prevent the application of pressure on the part. When a die temperature of 280 °C was reached, the stops were removed and 200 psi of pressure was applied. The temperature was raised to 315 °C over approximately 20 min and maintained for 1.5 h, after which time the die was allowed to cool to below 232 °C. At this temperature, it was taken out of the press, and the resin disk was removed. In all cases, a high-quality neat resin disk with minimum surface flaws was produced.

**(b) Plates.** The typical resin plate preparation was similar to that of the disks with the following modifications. The 10 cm  $\times$  10 cm die was charged with 25–30 g of molding powder. Upon reaching 280 °C, the nominal pressure applied depended on whether the samples were phthalic (500 psi) or nadic (550 psi) end capped. Phthalic end-capped samples were then ramped (rise time, 20 min) to 300 °C and held there for 15 min. The nadic-end-capped analogs were ramped to 315 °C followed by a 2 h dwell time. In either case, the die was then allowed to cool to 285 °C, and the piece was removed from the mold.

**(7) Aging for  $^{13}\text{C}$ -Labeling Study.** As noted in the Introduction, oxidation only occurs to a depth of 0.1–0.2 mm into the polymer surface.<sup>8,13</sup> To completely convert the neat resins (labeled and unlabeled) into oxidized polymer, the sample disks were ground to a fine powder before aging. The powders were spread in the bottom of a Petrie dish and loosely covered. Aging was carried out at 315 °C for 65 h in an oven under flowing air. The yellow-brown powders, which turned dark brown and lost about 15% weight during the aging, were oxidized throughout, as evidenced by microscopic FTIR.

**(8) Weight Loss Studies of Powders in Air.** The 10 cm  $\times$  10 cm neat resin plates were shattered with a hammer and then ground into a fine powder with a Spex Industries (Edison, NJ) 5300 Dual Mixer/Ball Mill. The resulting powder was sieved using a small sieve set (#3536). Only powder in the 200–100 mesh range was used for the aging study. The powders proved to be substantially hygroscopic, and in order to obtain accurate weight loss data, the following procedure was developed. Fifteen 5 mL glass vials were each filled with the milled powder (ca. 0.8 g) and dried in a 315 °C oven under

flowing air for 1 h. The weight at this point was set as the starting weight. Samples were then removed from the 315 °C oven at preset times, cooled in a desiccator, capped, and weighed again to determine weight loss. A preliminary control study determined that the weight loss observed upon aging in the glass vial was essentially the same ( $\pm 1\%$ ) as that observed when the powders were spread in the bottom of a Petri dish.

**(9) Weight Loss Studies of Powders in N<sub>2</sub>.** For aging carried out in nitrogen, 0.8 g samples were placed in glass ampules, dried, degassed, and sealed under N<sub>2</sub>. After the preset aging times, the ampules were removed, cooled in a desiccator, and then opened for weighing.

**(10) Microscopic FTIR.** Microscopic FTIR was done in reflectance mode on polished samples using a 740 Nicolet Bench with a NIC PLAN microscope attachment with a 4 cm<sup>-1</sup> spectral resolution and a gold-coated slide as background. The data were analyzed using OMNIC software.

**(11) NMR.** <sup>13</sup>C NMR spectra were obtained on a Bruker AM-300 spectrometer fitted with a high-power solids attachment and controlled by a TECMAG data system running MACNMR 5.1 software. Solid polymer samples were run using cross-polarization with magic angle spinning at 5 kHz (CP-MAS). The acquisition also employed spinning side-band suppression using a TOSS sequence. The spectra were externally referenced to the carbonyl of glycine (196.1 ppm relative to tetramethylsilane). Isotope-enriched spectra are shown as difference spectra obtained by subtracting the corresponding natural abundance spectrum, prepared and aged in the same way. Acquisition conditions were carefully matched between enriched and natural abundance samples. Consequently, the difference spectra contain only isotope-labeled resonance peaks.

## Results and Discussion

**(1) <sup>13</sup>C NMR Labeling Studies. (a) General.** Two different <sup>13</sup>C-enriched modifications of PMR-15, labeled as shown in Scheme 2, were prepared. In the first modification, we labeled the nadic end-cap at the methyne carbons  $\alpha$  to the carbonyl groups. Our choice of the end cap is based on the well-known observation that the aliphatic carbons of the nadic end cap disappear on oxidation.<sup>8g,h</sup> Indeed, for the nadic end cap a plethora of thermal-oxidative decomposition pathways are *a priori* feasible (*vide infra*). However, of the various possible positions on the end cap, we chose to tag those  $\alpha$  to the carbonyl groups because mechanistic considerations led us to believe that they would be the most likely to remain after initial degradation.

In our second modification, the CH<sub>2</sub> carbon of MDA was labeled. This carbon was chosen because, as noted in the Introduction, strong evidence suggests that the methylene is oxidized primarily to a carbonyl on aging in air.<sup>8</sup>

Having our labeled starting materials in hand, we now wanted to assure that we would obtain a maximal amount of oxidation product to study. We have noted above, however, that the outer surface (not the inside of the resin or the composite piece) is where oxidation occurs. Hence, we decided to mill pieces of cured polyimide to a fine powder, far smaller than the thickness of the typical oxidation layer. This powder was then isothermally aged. In this way, the polymer sample could be completely converted to oxidized material. To verify that this assumption was correct, a small sample of unlabeled PMR-15 powder, aged for 64 h, was mounted in epoxy, ground to reveal cross-sectional areas, and highly polished. The samples were analyzed by microscopic FTIR in reflectance mode in several areas. The use of a 100  $\mu$ m diameter analyzing area allowed us to examine different regions of the oxidized

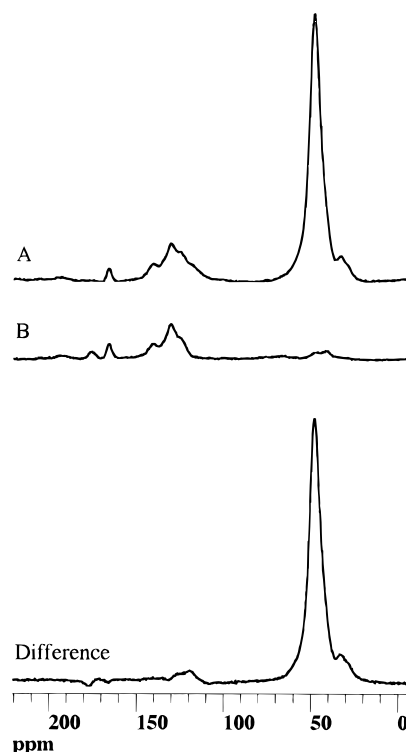


**Figure 1.** <sup>13</sup>C spectrum of (A) labeled PMR-15 powder; (B) natural abundance powder. (bottom) Difference spectrum showing only peaks due to the carbons labeled on the norbornyl end cap.

samples. FTIR microscope analysis showed the particles to be completely oxidized. The resulting FTIR spectrum was in good agreement with that of the outer oxidized layer from a sample aged for 1000 h at 343 °C from a previous study.<sup>8g,h</sup>

To focus in on the transformations occurring to the labeled carbons upon thermal oxidative aging, it was necessary at each step to determine the solid state <sup>13</sup>C NMR spectrum of a natural abundance milled PMR-15 powder, as well as that of the labeled analog. Because care was taken to match experimental conditions at each step, it was possible to subtract the unlabeled spectra from that of the labeled to give a difference spectrum showing only peaks for the labeled resonance. To demonstrate, an NMR spectrum of unaged, natural abundance PMR-15 powder is shown in Figure 1 (middle) along with that for the nadic <sup>13</sup>C-labeled PMR-15 powder (top). Subtraction of the unlabeled from the labeled spectrum gives the difference spectrum (bottom), which shows only the peak for the isotope-labeled carbons. Henceforth, all of the other spectra of <sup>13</sup>C-labeled polymers are shown as difference spectra.

**(b) Nadic End Cap.** The solid NMR difference spectra of nadic-labeled PMR-15 aged for up to 64 h indicate that, upon oxidation, nearly all the <sup>13</sup>C-labeled nadic peak at 48 ppm is consumed (see Figure 2). In its place three new broad peaks for labeled carbons grew in at 110–120, 125–140, and 155–165 ppm. (Another smaller broad peak at approximately 190 ppm, present in the 16 and 64 h samples, is a spinning side band of the aromatic peak and can be disregarded.) Though the spectrum is complex, these broad peaks suggest several possible degradation pathways, which are outlined in Scheme 3<sup>15</sup> (along with some predicted <sup>13</sup>C chemical shifts for the labeled carbon<sup>16</sup>).

The first (path a) might involve rearrangement of the norbornyl ring to a substituted maleimide (154 and 128

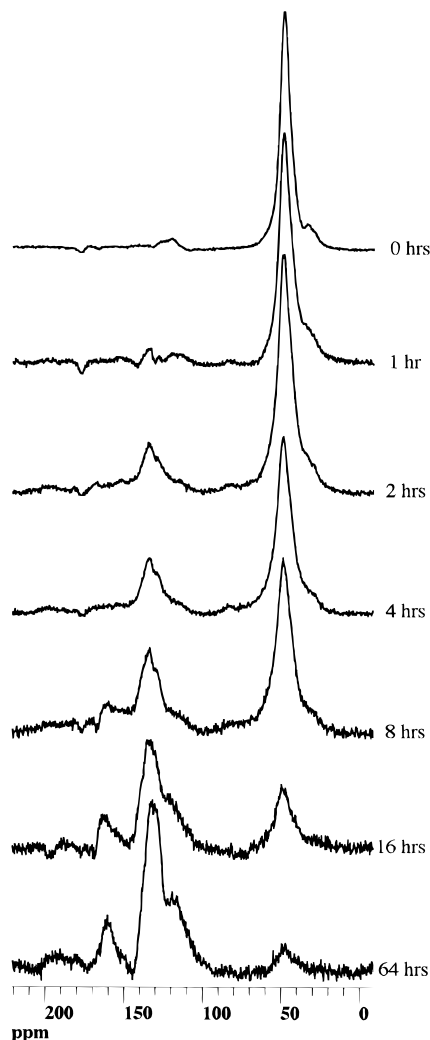


**Figure 2.** Difference spectra of PMR-15 powders  $^{13}\text{C}$ -enriched on the norbornyl end cap, shown as processed and after aging for up to 64 h.

ppm). Oxidative cleavage of the bond to the methylene of the norbornene (path b) moieties could lead to either quinone (156 ppm) or hydroquinone (118 ppm) structures. Alternatively, oxidation of the bridging methylene (path c) followed by carbon monoxide extrusion might lead to substituted phenyl rings (130 ppm). Aromatic structures like these have been proposed by Hay *et al.*<sup>17</sup> as arising from higher temperature polymerization (330 °C) of *N*-phenylnadimide for long cure times (12 h). Baeyer–Villager-type oxidation (path d) might lead to oxidative cleavage of the imide bond. This would give rise to structures with oxygen directly attached to the labeled carbons (149 and 152 ppm) and other labeled carbons (119 and 124 ppm). We are presently synthesizing a series of model compounds of some of the products suggested by these  $^{13}\text{C}$ -labeling studies.

**(c) MDA.** As noted above, the  $\text{CH}_2$  carbon of MDA was labeled because of the strong evidence indicating that on aging in air it is oxidized primarily to a carbonyl.<sup>8</sup> In a recent high-resolution (solution) NMR study, Milhourat–Hammadi and co-workers<sup>18</sup> observed the slow (5 days) autoxidation of the PMR-15 model compound, a hydrogenated MDA bis-nadimide, at 225 °C to the corresponding DABP analog. The authors attributed this oxidation to a classical free radical-chain mechanism leading to a hydroperoxide intermediate which decomposes to ketone. Attempts by these authors

to use NMR to observe the same transformation in PMR-15 proved unsuccessful, however, presumably because of the insolubility of the products.

NMR difference spectra before and after aging of the methylene-labeled PMR-15 are shown in Figure 3. It is obvious from these spectra that all of the methylene is consumed on oxidation. The major peak at 195 ppm can be assigned to the expected DABP derivative and possibly to a related aldehyde (see Scheme 4). Indeed, solid NMR of a sample of the DABP analog of PMR-15 (DABP-15; *vide infra*) reveals that the carbonyl absorption of the DABP moiety appears in a broad peak (together with the carbonyl of BTDA) centered at 194 ppm. Surprisingly, two other carbonyl peaks are also present in Figure 3: a peak at 160 ppm (presumably due to ester) and one at 172 ppm (attributable to a carboxylic acid). As outlined in Scheme 4 (which also contains some predicted  $^{13}\text{C}$  chemical shifts<sup>16</sup>), the formation of all three products can be rationalized as arising from the thermally labile hydroperoxide intermediate (not observed), via a variety of well-documented<sup>19</sup> homolytic and heterolytic decomposition pathways. Indeed, products, such as alcohols, carboxylic acids, and esters, have been observed in a study of the 200 °C oxidative degradation of a highly branched poly(phenylenemethylene).<sup>81</sup>

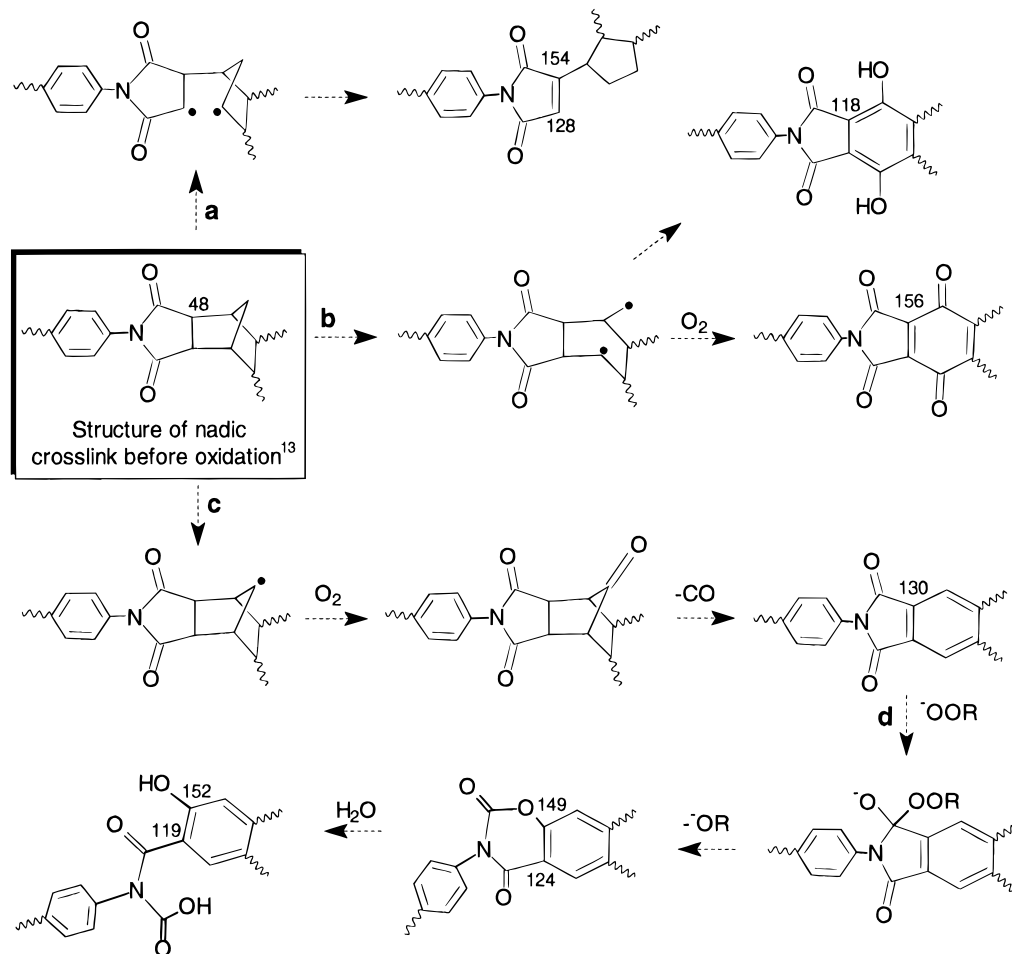
**(2) Weight Loss Study.** In the previous section, we have demonstrated that both the nadic end cap and the MDA methylene linkage undergo dramatic changes during aging. However, we have not yet determined which, if any, of these changes are responsible for the weight loss observed. To better understand the contribution of these transformations to weight loss, we prepared milled cured samples of PMR-15 and four analogs: (1) PMR-19, a PMR-15 analog with  $n = 3$  (formulated MW = 1943); (2) DABP-15, a nadic-end-capped polyimide with  $n = 2$  (formulated MW = 1501) in which the MDA has been replaced by DABP; (3) PAPMR-15, an analog of PMR-15 in which the nadic end cap is replaced by phthalic endcaps (formulated MW = 1427); and (4) PADABP-19, the phthalic-end-capped analog of PMR-19 (formulated MW = 1878). Samples of each of these powders were aged isothermally in air, and the weight loss results are recorded in Figure 4.

Studying the curves of Figure 4, we first observe the following order of decreasing weight loss: PMR-15 > DABP-15  $\approx$  PMR-19  $\gg$  PAPMR-15 > PADABP-19. This order and the relative spacing of the curves suggest that there are (at least) three separate mechanisms of weight loss in these systems.

The most rapid source of weight loss and the first mechanism we will focus on appears to stem from the degradation of the nadic group. This is evidenced by the large initial weight loss in nadic-end-capped PMR-15, DABP-15, and PMR-19. Figure 5 shows this initial weight loss for just the first 8 h for each of the curves shown in Figure 4. In this portion of the curves, the weight loss is effectively linear with respect to time. Using linear regression, the slope of these lines (the rate of initial weight loss) was calculated. This rate shows a strong linear correlation to the weight percent of nadic initially present in the polymer, but not on MDA, as evidenced by the plot in Figure 6. Clearly, as the relative amount of nadic decreases, so does the initial rate of weight loss.

Indeed, NMR evidence (Figure 7) supports this correlation. This figure shows the PMR-15 powder (natural abundance) aged for up to 120 h. As has been

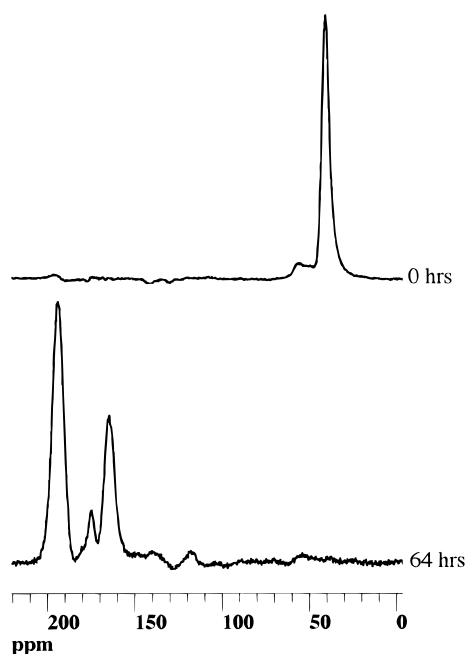
## Scheme 3. Possible Degradation Pathways and Products of the Nadic End Cap Moiety in PMR-15



previously observed,<sup>8h</sup> the peaks arising from the nadic cross-link (48 and 175 ppm) disappear on aging. In the natural abundance spectra of the powders, those peaks are essentially gone after only 6 h. In the more sensitive <sup>13</sup>C-labeled spectra (Figure 2), some peaks (e.g., 48 ppm) from the unoxidized cross-link are still present after 64

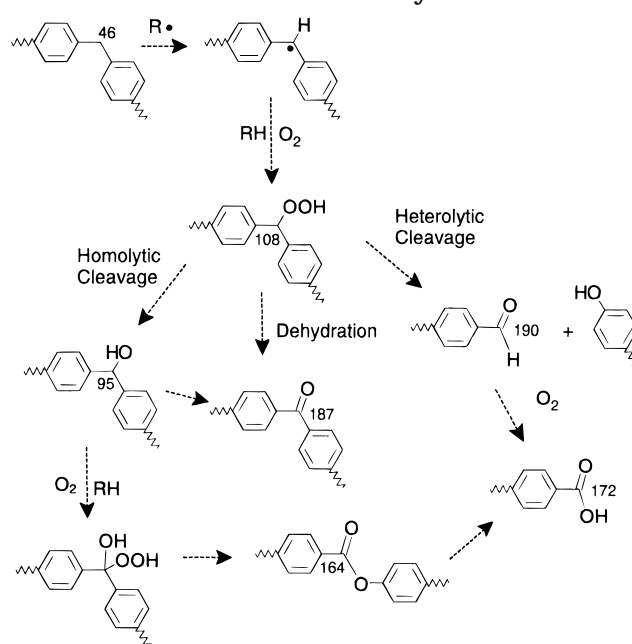
h. It should be noted that for powder samples aged up to 120 h in the absence of oxygen, solid NMR and FTIR spectra remain essentially unchanged. This indicates that the decomposition is clearly an oxidative process.

The second source of weight loss is the MDA moiety, which is reflected in the higher weight loss overall of



**Figure 3.** Difference spectra of PMR-15 powders <sup>13</sup>C-enriched on the MDA, shown before and after aging for 64 h.

## Scheme 4. Possible Degradation Pathways and Products of the MDA Moiety in PMR-15



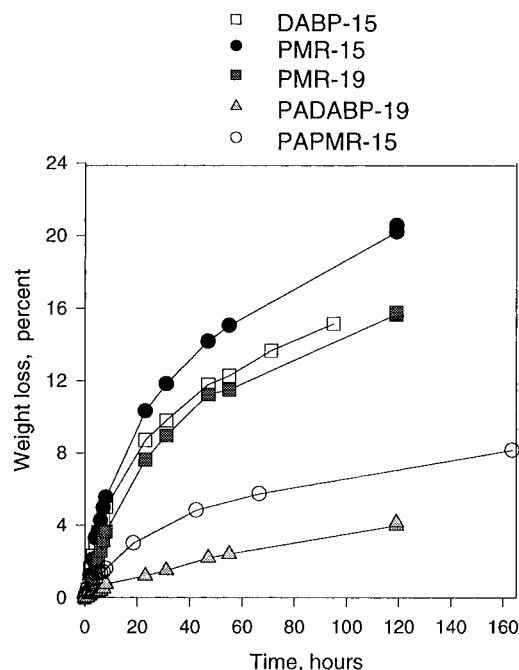


**Figure 4.** Weight loss of PMR-15 and derivatives aged as powders.

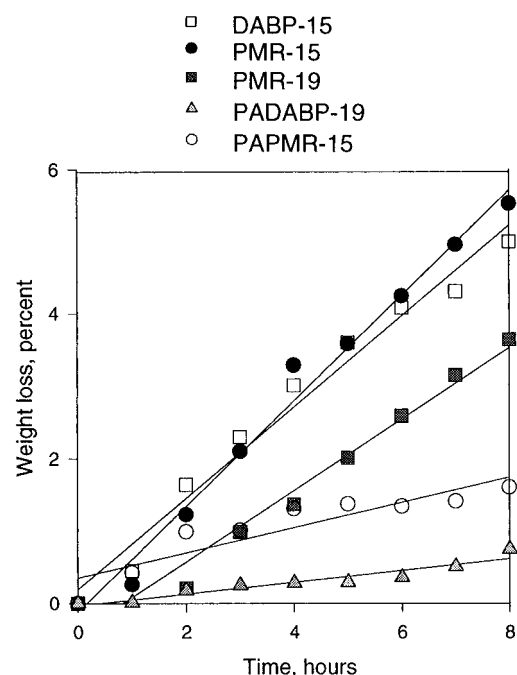


**Figure 5.** First 8 h of powder weight loss.

PMR resins as compared to the corresponding DABP compounds. Interestingly, the literature has argued<sup>8</sup> that the MDA in PMR-15 is simply oxidized to DABP. Natural abundance NMR spectra of the aging PMR-15 powders in Figure 7 compared to those of DABP-15 in Figure 8 support this argument. Both sets of spectra exhibit the rapid disappearance of the nadic peaks. The PMR-15 spectra also show disappearance of the methylene peak of MDA (42 ppm) and a shift of the aromatic peak at 141 ppm to lower field.<sup>20</sup> After a short time, both sets of spectra appear identical. FTIR spectra of the aged powders are in agreement with the nature and timing of these transformations.

However, if MDA were simply oxidized to DABP, then the weight loss of PMR-15 and DABP-15 should be the same.<sup>21</sup> Though very similar for the first 8 h (Figure

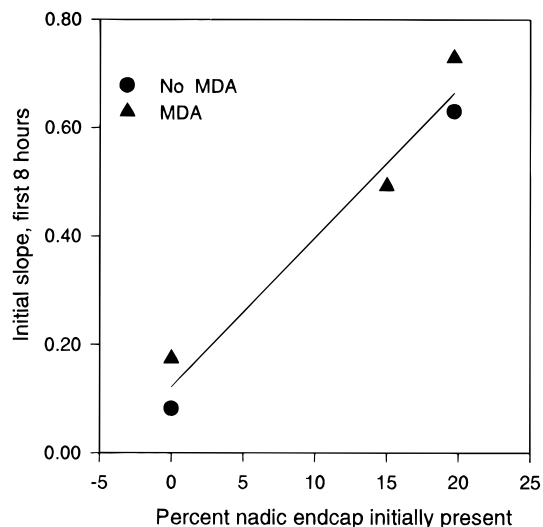


**Figure 6.** Plot of the rate of initial weight loss versus percent end cap present in the as-processed polymers.

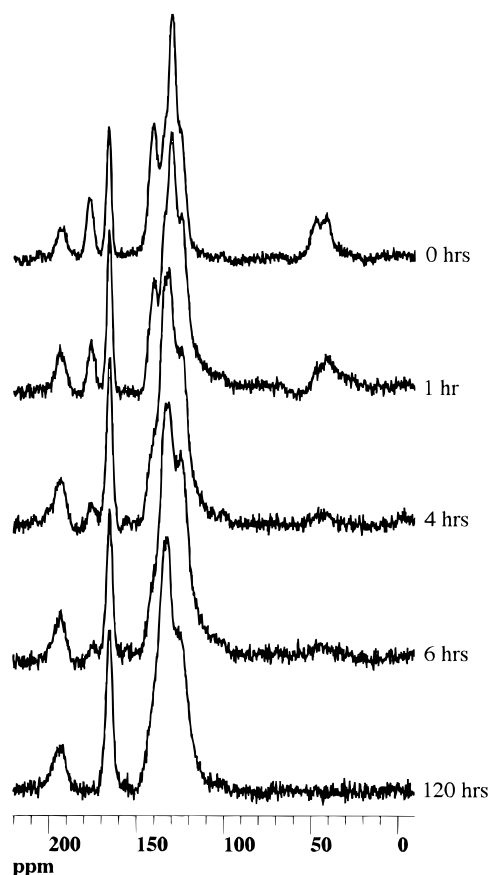


**Figure 7.** Natural abundance spectra of PMR-15 before aging and after up to 120 h in air at 315 °C.

5), for longer times (Figure 4) they are clearly very different. The above <sup>13</sup>C-labeling NMR studies make it apparent that the DABP moiety is not the only carbonyl being formed in the thermal oxidative degradation of PMR-15. Both an acid and an ester absorption are also detected (Figure 3). The formation of an acid from MDA would require a polymer strand cleavage. In addition, an ester would be expected to be substantially more labile (e.g., to hydrolysis) than the DABP ketone. We note as an aside that, despite the lower weight loss of DABP-15 as a powder, the insolubility and brittleness of this resin make it difficult to process and hence unsuitable as a commercial PMR-15 replacement.

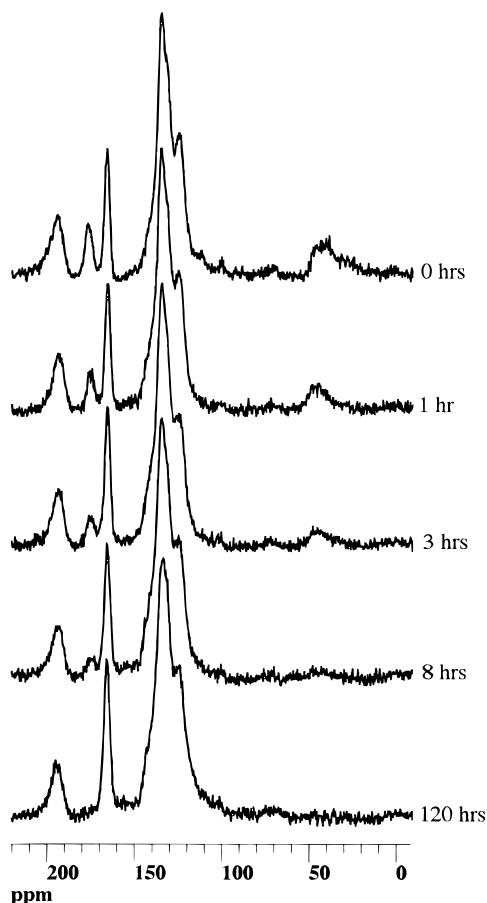


**Figure 8.** Natural abundance spectra of DABP-15 before aging and after up to 120 h in air at 315 °C.

The final mechanism observed for weight loss stems from the basic DABP/BTDA backbone. This weight loss is slow, as seen from the PADABP-19 curve, and little is known on the molecular level about the mechanism of this degradation. NMR of the natural abundance powders of PADABP-19 before aging and after 120 h of aging (Figure 9) shows relatively little change.  $^{13}\text{C}$  labeling of the carbonyls in both the backbone and the imide rings of BTDA would perhaps give insight into these reactions.

## Conclusions

$^{13}\text{C}$  labeling of selected sites in PMR-15 allowed for direct observation of the transformations arising from oxidation processes. As opposed to model compound studies, the reactions were followed directly in the polymer itself. In addition, the labeling provides the first evidence of the kinds of degradation reactions that are occurring in the end cap. Synthesis of several model compounds of the degradation products suggested by the labeling study are currently in progress.

Several PMR formulations containing moieties determined to be present after oxidation, as suggested by the  $^{13}\text{C}$ -labeling study, were synthesized. Weight loss, FTIR, and natural abundance NMR of these derivatives were followed during aging. In this way, weight loss was related to the observed transformations from the labeling study. Three separate mechanisms of weight loss were proposed: the weight loss originating from the rapid degradation of the nadic end caps, that arising from oxidation of the methylene carbons of MDA, and that proceeding from the much slower degradation of the BTDA moieties.

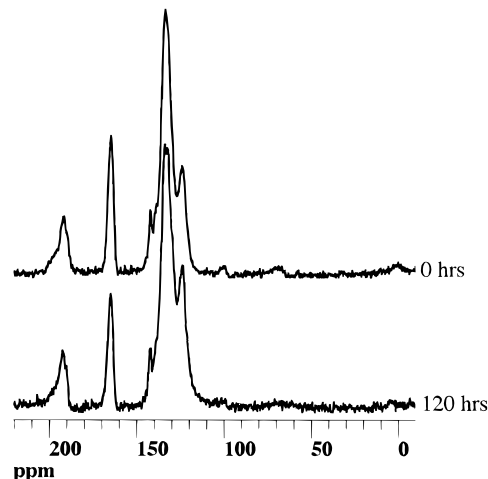


**Figure 9.** Natural abundance spectra of PADABP-19 before aging and after 120 h in air at 315 °C.

Additional studies will focus on the elucidation by  $^{13}\text{C}$ -labeling studies of the more subtle changes occurring in the interior of the polymer samples on postcure and aging. This is of importance, since some of these reactions are probably responsible for changes in physical properties, such as increasing glass transition temperature on postcure. They are also likely to contribute to embrittlement and microcracking in the interior of the samples in long-term use.

**Acknowledgment.** The authors would like to thank Mr. Dan Schiemann of NYMA Technologies for thermal analysis, Dr. Pilar Herrera-Fierro of the Ohio Aerospace Institute for microscopic FTIR, and Ms. Linda Ingraham of Gilchrist for carrying out the powder weight loss studies.

## References and Notes

- (1) Ethel and David Resnick chair in Active Oxygen Chemistry.
- (2) NRC/NASA Lewis Senior Research Associate, 1990–1996.
- (3) Serafini, T. T.; Delvigs, P.; Lightsey, G. R. *J. Appl. Polym. Sci.* **1972**, *16*, 905–915.
- (4) Meador, M. A.; Cavano, P. J.; Malarik, D. C. *Proceedings of the Sixth Annual ASM/ESD Advanced Composites Conference*, 1990; pp 529–539.
- (5) Serafini, T. T.; Vannucci, R. D.; Alston, W. B. Second Generation PMR Polyimides. NASA TMX-71894, 1976.
- (6) Vannucci, R. D.; Malarik, D. C.; Papadopoulos, D. S.; Waters, J. F. *Advanced Materials: Looking Ahead to the 21st Century*, Proceedings of the 22nd International SAMPE Technical Conference, Boston, Massachusetts, November 6–8, 1990; pp 175–185. Also NASA TM 103233.
- (7) Bowles, K. *Materials-Process: The Intercept Point*, Proceedings of the 20th International SAMPE Technical Conference, Minneapolis, Minnesota, September 27–29, 1988; pp 552–561. Also NASA TM 100922.
- (8) (a) Dine-Hart, R. A.; Wright, W. W. *Die Makrom. Chem.* **1972**, *153*, 237–254. (b) Jewell, R. A.; Sykes, G. F. In *Chemistry and Properties of Crosslinked Polymers*; Labana, S. S., Ed.; Academic Press: New York, 1977; pp 97–106. (c) Cf. Alston, W. B. *SAMPE J.* **1981**, March/April, 5–13. (d) Young, P. R.; Stein, B. A.; Chang, A. C. *Proc. 28th Int. SAMPE Symp.* **1983**, April 12–14, 824–837. (e) Young, P. R.; Chang, A. C. *Proc. 33rd Int. SAMPE Symp.* **1988**, March 7–10, 538–550. (f) Kuroda, S.; Mita, I. *Eur. Polym. J.* **1989**, *25*, 611–620. (g) Meador, M. A.; Lowell, C. E.; Johnston, J. C.; Cavano, P. J.; Herrera-Fierro, P. *HITEMP Review 1995: Advanced High Temperature Engine Materials Technology Program*; Gray, H. R.; Ginty, C. A., Eds.; NASA Conference Publication 10178, 1995; paper 8, pp 1–12. (h) Meador, M. A. B.; Lowell, C. E.; Cavano, P. J.; Herrera-Fierro, P. *High Perform. Polym.* **1996**, *8*, 363–379. (i) See also the related study on the thermal oxidative degradation of polybenzyl: Lady, J. H.; Kesse, I.; Adams, R. E. *J. Appl. Polym. Sci.* **1960**, 71–76.



- (9) For example, see: Sutter, J. K.; Jobe, J. M.; Crane, E. A. *J. Appl. Polym. Sci.* **1995**, *57*, 1491–1499.
- (10) (a) Frimer, A. A.; Cavano, P. J. *Polyimides: Materials, Characterization and Application*, Proceedings of The Fourth International Conference on Polyimides; Feger, C., Ed.; Society of Plastic Engineers: 1991; pp 17–20. Also NASA Technical Memorandum 105335, 1991, pp 1–5. (b) Frimer, A. A.; Cavano, P. J. In *HITEMP Review 1991: Advanced High Temperature Engine Materials Technology Program*; Gray, H. R., Ginty, C. A., Eds.; NASA CP-10082, 1991; pp 12-1 to 12-13. (c) Frimer, A. A.; Cavano, P. J.; Alston W. B.; Serrano, A. *HITEMP Review 1992: Advanced High Temperature Engine Materials Technology Program; Volume I: Overviews, Fan/Compressor Materials (Polymer Matrix Composites), and Fibers*; Gray, H. R., Ginty, C. A., Eds.; NASA Conference Publication 10104, 1992; pp 14-1 to 14-15. (d) Frimer, A. A.; Cavano, P. J. In *Advances in Polyimide Science and Technology*; Feger, C., Ed.; Technomic Publishing Co.: Lancaster, PA, 1993; pp 41–54. (e) Frimer, A. A.; Kinder, J. D.; Youngs, W. J.; Meador, M. A. *B. J. Org. Chem.* **1995**, *60*, 1658–1664. (f) Frimer, A. A.; Cavano, P. J.; Alston, W. B. *High Perform. Polym.* **1995**, *7*, 93–104.
- (11) (a) Ansari, A. A.; Turk, M. J.; Alston, W. B.; Frimer, A. A.; Scheiman, D. A. *HITEMP Review 1995: Advanced High Temperature Engine Materials Technology Program*; Gray, H. R., Ginty, C. A., Eds.; NASA Conference Publication 10178, 1995; paper 10, pp 1–11. (b) Turk, M. J.; Ansari, A. A.; Alston, W. B.; Frimer, A. A.; Scheiman, D. A. In preparation.
- (12) (a) Ahn, M. K.; Smirnov, A. I.; Smirnova, T. I.; Belford, R. L. *Macromolecules* **1995**, *28*, 7026. (b) Ahn, M. K.; Stringfellow, T.; Bowles, K. J.; Meador, M. A. *Mater. Res. Soc. Proc.—High Perform. Polym.* **1993**, *305*, 217–227. (c) Ahn, M. K.; Stringfellow, T.; Bowles, K. J.; Meador, M. A. *J. Polym. Sci., Part B* **1993**, *31*, 831–841. Ahn, M. K.; Weber, R. T.; Meador, M. A. B. *HITEMP Review, 1993: Advanced High Temperature Engine Materials Technology Program*; Gray, H. R., Ginty, C. A., Eds.; NASA CP-19117; p 20-1.
- (13) Bowles, K. J.; Jayne, D.; Leonhardt, T. A. *SAMPE Q.* **1993**, *24* (2), 2–9.
- (14) Swanson, S. A.; Fleming, W. W.; Hofer, D. C. *Macromolecules* **1992**, *25*, 582–588.
- (15) The structure of the norbornyl group after cross-linking was determined previously (Meador, M. A. B.; Johnston, J. C.; Cavano, P. J. *Macromolecules*, in press) to be mostly as shown in Scheme 3. For simplicity, we consider oxidation products from this structure only.
- (16) Calculations of the  $^{13}\text{C}$  NMR data were made using the ChemWindow3 (Softshell International)  $^{13}\text{C}$  NMR module developed by Dr. Erno Pretsch (ETH, Zurich). Synthesis of model compounds is underway.
- (17) Hay, J. N.; Boyle, J. D.; Parker, S. F.; Wilson, J. D. *Polymer* **1989**, *30*, 1032–1040.
- (18) Milhourat-Hammadi, A.; Gaudemer, F.; Merienne, C.; Gaudemer, A. *J. Polym. Sci., Part A: Polym. Chem.* **1994**, *32*, 1593–1597.
- (19) Frimer, A. A. *Chem. Rev.* **1979**, *79* (5), 359–387.
- (20) Milhourat-Hammadi and co-workers<sup>17</sup> observed that the aromatic carbon attached to the methylene appears at 141.2 ppm in a PMR-15 model compound and at 137.0 ppm in the corresponding DABP analog.
- (21) Actually, as noted above, the conversion of PMR-15 to DABP-15 should involve a weight gain.

MA970097I